Modified femtosecond pulse shaper using microlens arrays

K. M. Mahoney and A. M. Weiner

School of Electrical and Computer Engineering, Purdue University, West Lafayette, Indiana 47907-1285

Received November 28, 1995

We discuss a modified femtosecond pulse shaper that uses microlens arrays to convert the continuous band of frequencies normally obtained in the mask plane of a pulse shaper into a series of discrete spots. Our experiments demonstrate that this modification can improve pulse-shaping quality when modulator arrays with large interpixel gaps are used for Fourier-plane filtering. © 1996 Optical Society of America

Specially crafted femtosecond laser waveforms are of growing importance for many applications, such as optical communications, ultrafast spectroscopy, and high-field physics.[1] One powerful technique for femtosecond pulse shaping relies on spatial filtering in a zero-dispersion grating pulse compressor. Fixed microlithographically fabricated masks[2] as well as holograms,[3–5] moving mirrors,[6] and programmable devices such as pixelated one-dimensional liquid-crystal modulator arrays[7,8] and acousto-optic deflectors[9] have been used to implement the crucial spatial filtering function. Multiple-quantum-well self-electro-optic device arrays have also been used inside a pulse shaper to carve a femtosecond pulse into a number of separate wavelength channels for wavelength-division-multiplexed optical communications.[10] Self-electro-optic and other optoelectronic devices are attractive for modulator arrays because of their rapid reprogrammability ($>$100 Mbits/s); however, to achieve high speed these arrays must have small device cross-sectional areas, leading to low factors ($\sim$ 25% for the arrays used in Ref. 10) and large gaps. Although these gaps between the active pixels can be advantageous in wavelength-division multiplexing, they are undesirable in time-domain pulse-shaping applications. In this Letter we describe experimental tests of a modified pulse-shaper design that incorporates microlens arrays to reduce the effect of the interpixel gaps. Our modified pulse shaper can therefore be used to achieve high-quality pulse shaping even for low-fill-factor modulator arrays, such as two-dimensional liquid-crystal spatial light modulators and optoelectronic device arrays, although the effects of the interpixel gaps cannot be eliminated entirely.

In the conventional pulse-shaping geometry, a spatial phase or amplitude filter is used at the mask plane to produce a shaped output pulse, with the pulse shape given by the Fourier transform of the pattern transferred from the spatial filter onto the spectrum. This approach has been demonstrated to work very well as long as high-quality pulse-shaping masks are available. However, pixelated modulator arrays that have large interpixel gaps between the active regions are not compatible with the normal pulse-shaping geometry, because those frequencies hitting the dead spaces cannot be controlled. The idea of our modified design is to use microlens arrays to convert the continuous band of frequencies in the pulse shaper into a series of discrete spots corresponding to the active pixels of the modulator array. When incorporating these microlens arrays into the setup, one must be careful to keep the modified pulse-shaper dispersion free and to maintain the optical frequencies in the correct order so that they recombine into a single beam at the output.

We determined a geometry, shown in Fig. 1, that satisfies these requirements after performing a series of computer simulations using 4×4 ray-pulse matrices for dispersive optical systems.[11] The layout is similar to that of the conventional pulse shaper with the addition of the four microlens arrays configured as two pairs of telescopes inserted into the center of the pulse shaper. As in the conventional pulse shaper, the frequency components are spread out in a continuous band at the focus of the first bulk lens. The first microlens array takes the continuous band of light and converts it into a series of discrete spots (one discrete spot per microlens). The second microlens array changes the discrete spots back into a continuous band of frequencies. The first two microlens arrays form a telescope that reverses the positions of the various frequencies passing through an individual microlens. Therefore a second telescope (made up of the third and fourth microlens arrays) is needed to transpose the frequencies again and reposition them in the same order that they were in before the first microlens array. This allows the second bulk lens and grating to recombine all the frequency components into a single output beam propagating in a single, well-defined direction. The first and the second microlens arrays are separated by twice the microlens focal length (as are the third and the fourth arrays), and the total length from the focus of the first bulk lens to the focus

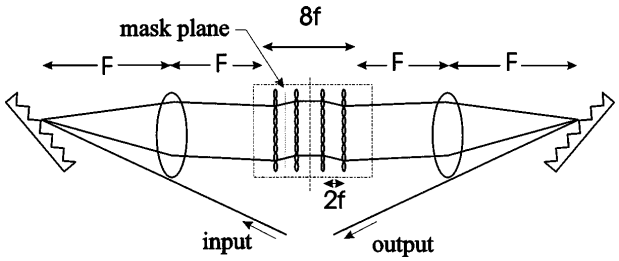

Fig. 1. Schematic of a modified pulse shaper that uses microlens arrays. The microlens arrays are separated by twice the microlens focal length (f) and the grating-to-bulk-lens spacing is the bulk-lens focal length (F).

0146-9592/96/110812-03$10.00/0

of the second bulk lens is eight times the microlens focal length. The mask plane is between the first and the second (or equivalently, between the third and the fourth) microlens arrays. As in the conventional pulse shaper, the shape of the output pulse is given by the Fourier transform of the spectrum as filtered at the mask plane.

In the actual experiments, we implemented the modified pulse shaper by using a reflection geometry version of Fig. 1. Because the layout in Fig. 1 is symmetric, a mirror can be placed at the symmetry plane located between the second and the third microlens arrays. This simplifies the alignment procedure and reduces the component count. The frequencies are spread out along the first microlens array, which focuses them to a series of discrete spots. The second microlens array converts the frequencies back to a continuous band. The mirror then retroreflects the various frequencies back through the system. We performed experiments testing this setup, using a colliding pulse mode-locked[12] (CPM) dye laser that produced sub- 100-fs pulses at a wavelength of 620 nm. We used an 1800 line/mm grating, a bulk lens with a 150-mm focal length, and microlens arrays fabricated by United Technologies Adaptive Optics Associates (AOA-0100-1.7-S) that were arranged in a two-dimensional 6.8 mm $\times$ 6.8 mm square array with 100-μm center-to-center spacing, $>$98% fill factor, and a focal length of 1.7 mm. Note that our experiments actually use only a single row on each of the two-dimensional microlens arrays.

Initially, we measured the output pulses from the two pulse shapers without any filter at the mask plane. Intensity cross-correlation measurements of the output pulses from the conventional and the modified pulse shapers were taken with an ultrashort pulse directly from the CPM laser as a reference. The output pulses are 87 and 95 fs FWHM, respectively, assuming secant hyperbolic pulse shapes. The output pulse widths are comparable with the input pulse widths; the difference between 87 and 95 fs is within the day-to-day variation of our CPM laser pulse width (the two measurements were performed on different days). Thus we have satisfied the requirement that the pulse shaper must remain dispersion free.

Although the pulse itself is not broadened, a pair of sidelobes is observed in the output pulse shape from the modified pulse shaper that are not present with the conventional pulse shaper (for one representative plot see Fig. 2). The sidelobes are located at $\pm$4.4 ps and typically have an intensity of $\sim$5$-$12% that of the main pulse at $t = 0$, depending on the precise alignment of the microlens arrays. These sidelobes are caused by optical frequency components hitting the border between two adjacent microlenses. Unlike in our ray-tracing analysis, in the real experiment with finite Gaussian beams diffraction effects will cause those frequency components straddling a pair of microlenses to scatter out of the main beam. This leads to a periodic series of dips in the output spectrum with a frequency separation

$$\Delta f = \frac{cd\cos\theta_d}{\lambda^2 F}\,\Delta x\,,$$

where d is the grating period, $\theta_d = 35°$ is the output angle for the first diffraction grating, F is the focal length of the bulk lens, c and λ are the speed of light and the wavelength, respectively, and $\Delta x = 100$ μm is the microlens period. For these experimental parameters $\Delta f = 2.37$ THz, corresponding to a sidelobe separation of 4.2 ps, in good agreement with the data.

Our next goal was to test the ability of the modified pulse shaper to correct for dead space in pixelated masks. Therefore we designed and fabricated a series of fixed-amplitude masks that mimic pixelated modulator arrays with varying amounts of interpixel dead space. Each mask consists of a 1.5-mm window that passes 4.54 nm of optical bandwidth. This is narrower than the bandwidth of the CPM laser and demonstrates simple pulse shaping by spectral windowing of the input pulse to produce a broadened output pulse. Each mask contains a series of clear areas that transmit light separated by opaque regions, corresponding to active pixels and dead spaces, respectively. Each of the masks is intended to mimic a modulator array with different amounts of interpixel dead space. One mask has clear areas that are 50 μm wide, with 50-μm opaque regions. The other four masks have 70/30-, 80/20-, 90/10-, and 100/0-μm clear and opaque regions, respectively. All the pixels are spaced at 100 μm, a width that was designed to match the period of the microlenses in the arrays. The 1.5-mm window is narrower than the width of microlens array, so the light passes through only the 15 microlenses that are aligned with the corresponding pixels. Our intent is that the modified pulse shaper should direct frequency components away from the opaque regions and therefore produce shaped pulses similar to that corresponding to a clear window with no opaque regions.

Figure 3 shows a comparison of output pulse-shape data generated by intensity cross correlation for the conventional [Fig. 3(a)] and the modified [Fig. 3(b)] pulse shapers, with the 90/10, 80/20, 70/30, and 50/50 masks (the 100/0 results for the modified pulse shaper are similar to that shown in Fig. 2 but with

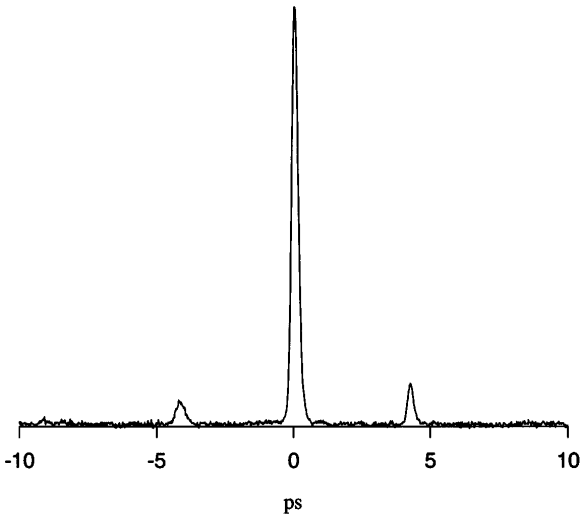

Fig. 2. Cross correlations of the output pulses emerging from the modified pulse shaper without any filtering of the frequency spectrum.

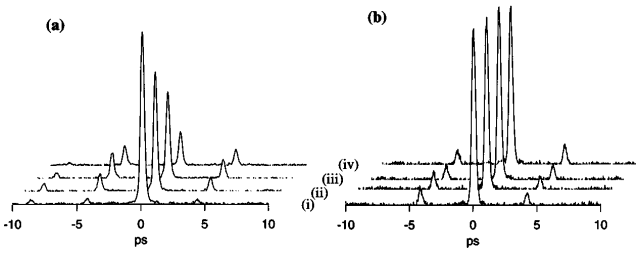

Fig. 3. Cross correlations of the output pulses from the (a) conventional and (b) modified pulse shapers. The waveforms produced with a mask that has (i) 90-μm pixels with a 10-μm gap, (ii) 80-μm pixels/20-μm gap, (iii) 70-μm pixels/30 μm gap, and (iv) 50-μm pixels/50-μm gap are shown.

some broadening of the main pulse at $t = 0$, as expected). The main pulses shown in Fig. 3 are also temporally broadened because of the spectral windowing. We observe that as the dead space increases in the conventional pulse shaper, the height of the central peak decreases dramatically. The decrease in intensity arises both because of energy being blocked by dead space in the spatial mask and because of redistribution of energy to subsidiary peaks, which grow relative to the main peak as the dead space increases. In our most extreme case (50 μm clear and 50 μm opaque, or 50% fill factor), we observe that the sidelobe heights for the conventional pulse shaper [Fig. 3(a), curve (iv)] have grown to 40–50% of the desired central peak at $t = 0$. For the modified pulse shaper, however, the intensity of the main peak at $t = 0$ remains essentially constant, as do the intensities of the low-level sidelobes ($\sim$10–12% relative to the main peak). This confirms our idea that the modified pulse shaper can improve the output pulse shape by avoiding the opaque regions corresponding to interpixel dead space. For the 90/10 mask, the relative heights of the sidelobes for the modified pulse shaper [Fig. 3(b), curve (i)] are actually higher than for the conventional pulse shaper [Fig. 3(a), curve (i)]. For the 80/20 mask, however, the sidelobes for the modified pulse shaper [Fig. 3(b), curve (ii)] are lower than for the conventional pulse shaper [Fig. 3(a), curve (ii)]. Therefore for our experimental parameters the effective clear aperture, determined by the scattering from the edges of individual microlenses, is approximately 85 out of 100 μm (despite the fact that the actual microlens fill factor is nearly 100%). The 85-μm effective aperture of the microlens array is the reason behind the sidelobe heights at $\pm$4.2 ps. One can adjust the effective aperture by increasing or decreasing the input beam diameter. But any decrease in spot size at the microlens array (which would reduce the amount of scattering at the edges of the individual microlenses) is traded off for an increase in spot size at the amplitude mask. Therefore one cannot arbitrarily choose the optimum input spot size without considering the resulting spot size at the microlens array and the mask plane. Nevertheless our data clearly show that for masks or modulator arrays with large interpixel dead spaces the modified pulse shaper can provide a dramatic improvement over the conventional pulse shaper. For nonpixelated modulators, or modulators with very large fill factors, the conventional pulse shaper is of course preferred.

In conclusion, we have demonstrated a modified pulse shaper that uses microlens arrays to convert the continuous band of frequencies normally obtained at the mask plane into a series of discrete spots. This modification should improve the pulse-shaping quality that can be obtained with pixelated modulators with large interpixel gaps. Our results should open up new opportunities for programmable generation of space–time images with two-dimensional spatial light modulators and for modulation of femtosecond waveforms at gigabit per second rates by the use of optoelectronic device arrays for optical communications and optical information processing.

The authors thank Adaptive Optics Associates for the use of the microlens arrays. This research was supported in part by the National Science Foundation under grant ECS-9312256 and by U.S. Air Force Office of Scientific Research grant F49620-95-1-0533.

References

1. A. M. Weiner, Prog. Quantum Electron. **19,** 161 (1995).
2. A. M. Weiner, J. P. Heritage, and E. M. Kirschner, J. Opt. Soc. Am. B **5,** 1563 (1988).
3. A. M. Weiner, D. E. Leaird, D. H. Reitze, and E. G. Paek, IEEE J. Quantum Electron. **28,** 2251 (1992).
4. M. C. Nuss and R. L. Morrison, Opt. Lett. **20,** 740 (1995).
5. K. Ema and F. Shimizu, Jpn. J. Appl. Phys. **29,** 631 (1990).
6. K. F. Kwong, D. Yankelevich, K. C. Chu, J. P. Heritage, and A. Dienes, Opt. Lett. **18,** 558 (1993).
7. A. M. Weiner, D. E. Leaird, J. S. Patel, and J. R. Wullert II, IEEE J. Quantum Electron. **28,** 908 (1992).
8. M. M. Wefers and K. A. Nelson, Opt. Lett. **18,** 2032 (1993).
9. C. W. Hillegas, J. X. Tull, D. Goswami, D. Strickland, and W. S. Warren, Opt. Lett. **19,** 737 (1994).
10. E. A. De Souza, M. C. Nuss, W. H. Knox, and D. A. B. Miller, Opt. Lett. **20,** 1166 (1995).
11. A. G. Kostenbauder, IEEE J. Quantum Electron. **26,** 1148 (1990).
12. J. A. Valdmanis, R. L. Fork, and J. P. Gordon, Opt. Lett. **10,** 131 (1985).